

Formation of wormholes by dark matter in the galaxy Dragonfly 44

Sayeedul Islam, Farook Rahaman, Ali Övgün, and Mustafa Halilsoy

Abstract: Recently, the ultra-diffuse galaxy (UDG) Dragonfly 44 in the Coma Cluster was observed and observations of the rotational speed suggest that its mass is almost the same as the mass of the Milky Way. On the other hand, interestingly, the galaxy emits only 1% of the light emitted by the Milky Way. Thus, astronomers reported that Dragonfly 44 may be made almost entirely of dark matter. In this study we try to determine whether or not the dark matter that constitutes Dragonfly 44 can form a wormhole. Two possible dark matter profiles are used, namely, UDG King's model and generalized Navarro-Frenk-White (NFW) dark matter profile. We have shown that King's model dark matter profile does not manage to provide a wormhole whereas the generalized NFW dark matter profile manages to find wormholes.

Key words: wormhole, dark matter, ultra-diffuse galaxy, Dragonfly 44, NFW dark matter profile.

Résumé : Récemment, les observations de la galaxie ultra-diffuse (UDG) Dragonfly 44 dans l'amas de Coma suggèrent que sa vitesse de rotation correspond à une masse qui est presque celle de la Voie Lactée. D'autre part, il est intéressant de noter que sa luminosité est seulement 1 % de celle émise par la Voie Lactée. Il s'ensuit que les astronomes rapportent que Dragonfly 44 peut être faite presque entièrement de matière noire. Nous étudions ici la possibilité que la matière noire constituant Dragonfly 44 peut créer un trou de ver ou non. Nous utilisons deux profils possibles pour cette matière noire, nommément, le modèle de UDG de King et le profil généralisé de matière noire de Navaro-Frank-White (NFW). Il ressort que le profil de King ne parvient pas à générer un trou de ver, mais que le profil de NFW est capable de générer un trou de ver. [Traduit par la Rédaction]

Mots-clés : trou de ver, matière noire, galaxie ultra-diffuse, Dragonfly 44, profil de matière noire de NFW.

1. Introduction

Today, one of the challenging questions in theoretical physics is the question of the existence of traversable wormholes [1–21]. Another mystery in physics is dark matter (DM) [22–24]. Like black holes, there is another miraculous type of object in our universe: wormholes. After the prediction of Einstein–Rosen bridges in 1935 [1], with a lot of theoretical evidence, researchers have proposed the existence of wormholes in space–time that act like shortcut paths to travel between any two widely separated or infinite regions of the universe or between another universes in a multi-universe model. Structurally, a wormhole looks like a tunnel (called its throat) with two mouths (most likely spheroidal). Here the most interesting thing is that the exotic matter needed to open its throat violates null energy conditions [2–4]. The curiosity about wormhole physics has vigorously increased since publication of Morris and Thorne's research article where they proposed the prospect of the existence of traversable wormholes as a solution of Einstein's field equations that does not contain an event horizon, and a traveler can easily move in both the regions in space–time through its straight stretch throat [2, 3]. By the existence of these hypothetical objects one could realize time machines or shortcuts among faraway regions of space.

The majority of the mass of the universe is thought to be made up of a most mysterious substance that does not interact with the electromagnetic force (i.e., cannot absorb, reflect or emit light):

DM whose nature and composition remain an overall question mark [22, 23]. Researchers hypothesize the existence of dark matter only from its gravitational effect. Observation of the spiral galaxy rotation curves is an enthralling experimental evidence for the existence of DM. The DM candidate particles are generally classified into cold, warm, and hot categories. Interaction of a scalar field whose energy density is dark energy may be caused by the DM particle mass. Over several decades it has been openly accepted that almost every galaxy contains a large amount of non-luminous matter forming massive DM halos around the galaxy based on different lines of evidence like flat rotation curves of spiral galaxies [24] and strong lensing system [25].

The model under consideration predicts that the ultra-diffuse galaxies' (UDGs) space distribution for 90 globular clusters observed around Dragonfly 44 [27] has the space density as follows

- Using a King's model-like approach [28, 29]:

$$\rho(r) \propto \kappa \left(\frac{r^2}{r_0} + \lambda \right)^\eta \quad (1)$$

where η , κ , r_0 , and λ are parameters. We assume that the averaged relative speed of the galaxies in the Coma cluster is

Received 1 November 2017. Accepted 17 January 2018.

S. Islam and F. Rahaman. Department of Mathematics, Jadavpur University, Kolkata 700032, West Bengal, India.

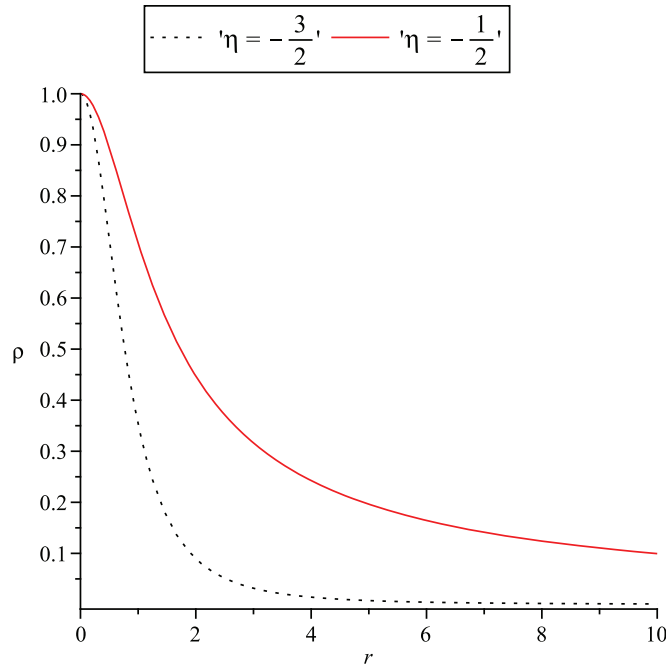
A. Övgün. Instituto de Física, Pontificia Universidad Católica de Valparaíso, Casilla 4950, Valparaíso, Chile; TH Division, Physics Department, CERN, CH-1211 Geneva 23, Switzerland; Physics Department, Arts and Sciences Faculty, Eastern Mediterranean University, Famagusta, North Cyprus via Mersin 10, Turkey.

M. Halilsoy. Physics Department, Arts and Sciences Faculty, Eastern Mediterranean University, Famagusta, North Cyprus via Mersin 10, Turkey.

Corresponding author: Sayeedul Islam (email: sayeedul.jumath@gmail.com).

Copyright remains with the author(s) or their institution(s). Permission for reuse (free in most cases) can be obtained from [RightsLink](https://rightslink.com).

Fig. 1. ρ versus r ($\kappa = 1$, $\lambda = 1$, and $r_0 = 1$). [Colour online.]



approximately equal to the velocity dispersion in the cluster $v \cong 1000$ km/s. This density profile is shown in Fig. 1.

- Using a generalized Navarro–Frenk–White (NFW) profile [26]:

$$\rho(r) \propto \frac{1}{r^\gamma [1 + (r/r_0)]^{3-\gamma}} \tag{2}$$

where γ and r_0 are parameters.

This paper is organized as follows. Section 2 introduces the traversable wormholes and their basic equations. In Sects. 3 and 4, we study the possibility of wormholes in the Dragonfly 44 galaxy by using the UDGs DM profile [27–29] and NFW DM profile [26], respectively. Finally, in Sect. 5, we present our remarks.

2. Wormhole formulation

The traversable wormhole space–time is given by the following [2, 3]:

$$ds^2 = -e^{2f(r)} dt^2 + \left[1 - \frac{b(r)}{r}\right]^{-1} dr^2 + r^2(d\theta^2 + \sin^2 \theta d\phi^2) \tag{3}$$

It is noted that $b(r)$ and $f(r)$ stand for the spatial shape function and the redshift function, respectively. The range of the radial coordinate is from $+\infty$ to $b(r_0) = r_0$ where r_0 is the minimum value of r (throat of the wormhole).

The Einstein field equations are given by

$$G_\nu^\mu = 8\pi T_\nu^\mu \tag{4}$$

where T_ν^μ and G_ν^μ are the stress–energy tensor and the Einstein tensor, respectively. Then one can calculate the nonzero Einstein tensors

$$G_t^t = \frac{b'}{r^2} \tag{5}$$

$$G_r^r = \frac{-b}{r^3} + 2\left(1 - \frac{b}{r}\right)\frac{f'}{r} \tag{6}$$

$$G_\theta^\theta = \left(1 - \frac{b}{r}\right)\left\{f'' + f'^2 + \frac{f'}{r} - \left(f' + \frac{1}{r}\right)\left[\frac{b'r - b}{2r(r - b)}\right]\right\} \tag{7}$$

$$G_\phi^\phi = G_\theta^\theta \tag{8}$$

where a prime indicates d/dr .

DM is generally defined in the form of general anisotropic energy–momentum tensor

$$T_\nu^\mu = (\rho + p_r)u^\mu u_\nu + p_r g_\nu^\mu + (p_t - p_r)\eta^\mu \eta_\nu \tag{9}$$

where $u^\mu u_\mu = -(1/2)\eta^\mu \eta_\mu = -1$. Note that p_t stands for the transverse pressure, p_r is the radial pressure, and ρ is the energy density. A possible set of u^μ and η^μ are given by $u^\mu = (e^{2f(r)}, 0, 0, 0)$ and $\eta^\mu = (0, 0, 1/r, (1/r)\sin\theta)$. Then the stress–energy tensors T_ν^μ are calculated as follows:

$$T_t^t = -\rho \tag{10}$$

$$T_r^r = p_r \tag{11}$$

$$T_\theta^\theta = T_\phi^\phi = p_t \tag{12}$$

3. Wormholes with the UDG King’s model DM

One can find the tangential velocity from the flat rotation curve for the circular stable geodesic motion in the equatorial plane as [21]

$$v^\phi = \sqrt{rf'} \tag{13}$$

which is responsible to fit the flat rotational curve for the DM. Rahaman et al. observe the rotational curve profile in the DM region as follows [19, 20]:

$$v^\phi = \alpha r \exp(-k_1 r) + \beta [1 - \exp(-k_2 r)] \tag{14}$$

where α , β , k_1 , and k_2 are constant positive parameters.

Using (13) and (14), the redshift function is obtained as follows:

$$f(r) = -\frac{\alpha^2 r}{2k_1 \exp(2k_1 r)} - \frac{\alpha^2}{4k_1^2 \exp(2k_1 r)} - \frac{2\alpha\beta}{k_1 \exp(k_1 r)} + \frac{2\alpha\beta \exp(-k_1 r - k_2 r)}{k_1 + k_2} + \beta^2 \ln(r) + 2\beta^2 E_i(1, k_2 r) - \beta^2 E_i(1, 2k_2 r) + D \tag{15}$$

where E_i and D are the exponential integral and integration constant, respectively. At large scales, it becomes $\exp(2f(r)) = B_0 r^{4v^\phi}$.

Now we discuss two cases for different values of the parameter η by using UDGs King’s DM profile for the stability of wormholes in the galaxy Dragonfly 44.

3.1. Case 1

For the UDGs King’s DM density profile [27–29]

$$\rho(r) = \kappa \left[\left(\frac{r}{r_0}\right)^2 + \lambda \right]^\eta \tag{16}$$

Fig. 2. $b(r)/r$ versus r ($r_0 = 1, \kappa = 1, \lambda = 1,$ and $\eta = -1/2$). [Colour online.]

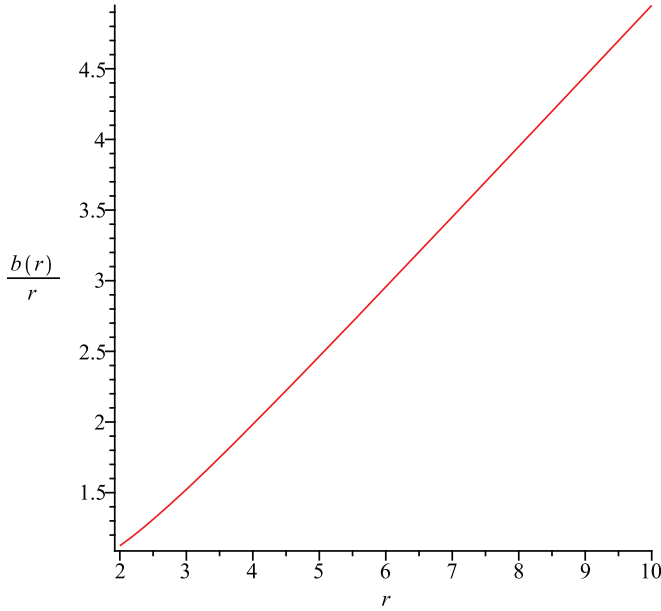
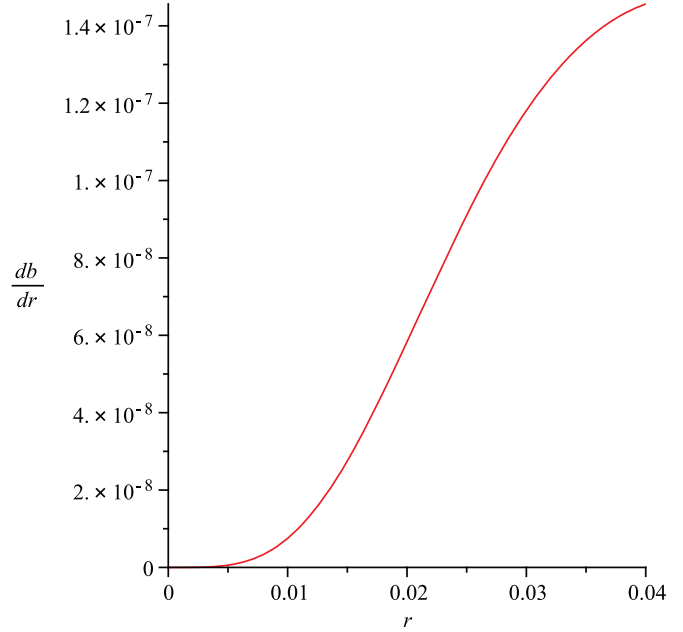


Fig. 3. $b'(r)$ versus r ($r_0 = 0.001$). [Colour online.]



we assume in this case $\kappa = 1, \lambda = 1,$ and $\eta = -3/2$. After one uses (13) and (14) and the UDG's DM density profile under the Einstein field equations, the shape function is calculated ($8\pi = 1$) as (see Fig. 2)

$$b(r) = \frac{r_0^2}{8(r^2 + r_0)} + \frac{r_0^{3/2}}{8} \tan^{-1}\left(\frac{r}{\sqrt{r_0}}\right) - \frac{r_0^3 r}{4(r^2 + r_0)^2} + C \quad (17)$$

Note that C is the integration constant and it is chosen as

$$C = r_0 - \frac{r_0^2}{8(1 + r_0)} + \frac{r_0^{3/2}}{8} \tan^{-1}(\sqrt{r_0}) + \frac{r_0^2}{4(1 + r_0)^2} \quad (18)$$

to satisfy the condition of $b(r_0) = r_0,$ then the flare-out condition ($b' < 1$) is checked, where r_0 is the radius of the throat

$$b' = \rho r^2 = \frac{r_0^3 r^4}{(r^2 + r_0)^3} \quad (19)$$

which is satisfied (see Fig. 3).

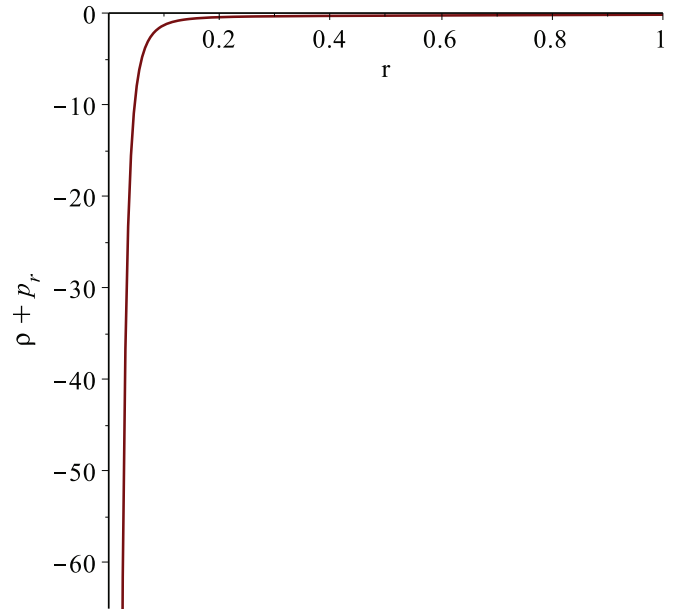
Furthermore from (10) the second derivative of b with respect to r is calculated as

$$b'' = -\frac{2r_0^3 r(2r^2 - r_0)}{(r^2 + r_0)^4} \quad (20)$$

The radial of pressure is shown as follows by substituting $f(r)$ and $b(r)$ into the solution (5)-(12):

$$p_r = \frac{-b}{r^3} + 2\left(1 - \frac{b}{r}\right)\frac{f'}{r} \quad (21)$$

Fig. 4. Null energy condition for case 1 ($r_0 = 0.001, \kappa = 1, \lambda = 1,$ and $\eta = -3/2$). [Colour online.]



$$f' = \frac{\alpha}{2r} [\exp(k_1 r)]^2 - 2\alpha\beta \exp[-r(k_1 + k_2)] + 2\frac{\alpha\beta}{\exp(k_1 r)} + \frac{\beta^2 \exp(-2k_2 r)}{r} - 2\frac{\beta^2 \exp(-k_2 r)}{r} + \frac{\beta^2}{r} \quad (22)$$

It is shown in Figure 4 that the null energy condition ($\rho + p_r < 0$) is violated so that one of the essential conditions for a wormhole is satisfied. However, the most important criterion for a wormhole, namely, $b(r)/r < 1$ is violated (see Fig. 2). So in this case a wormhole does not exist.

Fig. 5. $b'(r)$ versus r ($r_0 = 1$). [Colour online.]

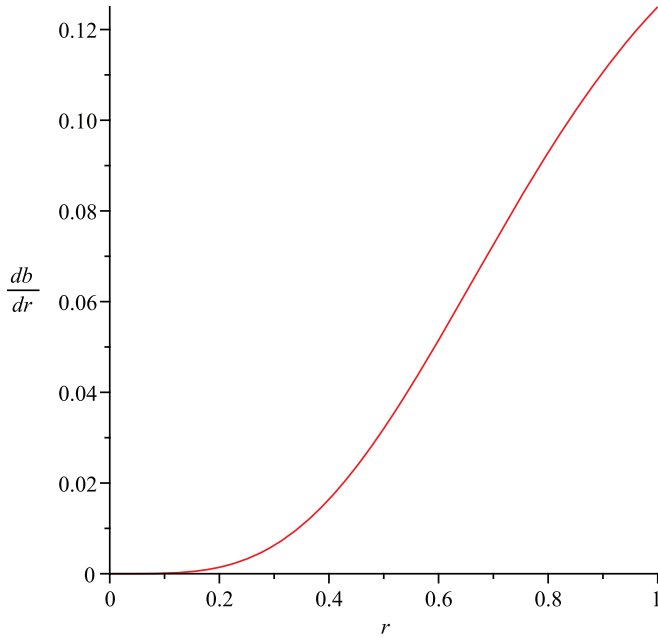
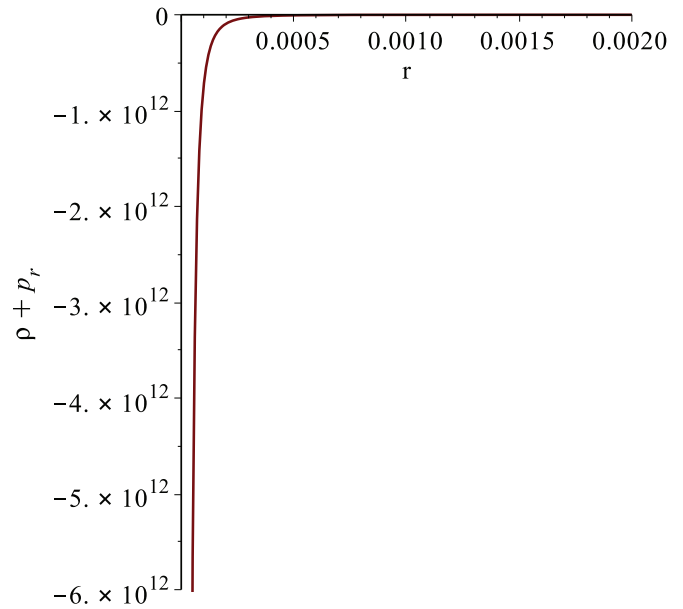


Fig. 6. Null energy condition for case 2 ($r_0 = 1, \kappa = 1, \lambda = 1,$ and $\eta = -1/2$). [Colour online.]



3.2. Case 2

In this section we follow the same method used in case 1 and the shape function is calculated.

The flare-out condition ($b' < 1$) is checked and found to be satisfied and plotted in Fig. 5.

It is also showed in the Fig. 6 that the null energy condition ($\rho + p_r < 0$) is violated as needed to hold a wormhole. However, as in case 1, $b(r)/r < 1$ is violated (see Fig. 7), so in this case a wormhole does not exist. Thus King’s model DM profile that constitutes Dragonfly 44 does not manage to provide a wormhole. Now we will determine whether or not generalized NFW DM profile that constitutes Dragonfly 44 manages to provide wormhole.

4. Wormholes with the NFWs DM

In this section we describe the DM halo distribution using the following generalized NFW profile for the existence of wormholes in the galaxy Dragonfly 44:

$$\rho(r) = \frac{1}{r^\gamma [1 + (r/r_0)]^{3-\gamma}} \tag{23}$$

In this expression, γ is the inner slope of the profile ($\gamma = 1$ corresponds to the case of a standard NFW profile), and r_0 is the scale radius and taking variation constant as unity.

Here we have discussed three different cases for the several values of the parameter γ .

4.1. Case 1

In this case we assume $r_0 = 10, \rho_0 = 0.05,$ and $\gamma = 3.$

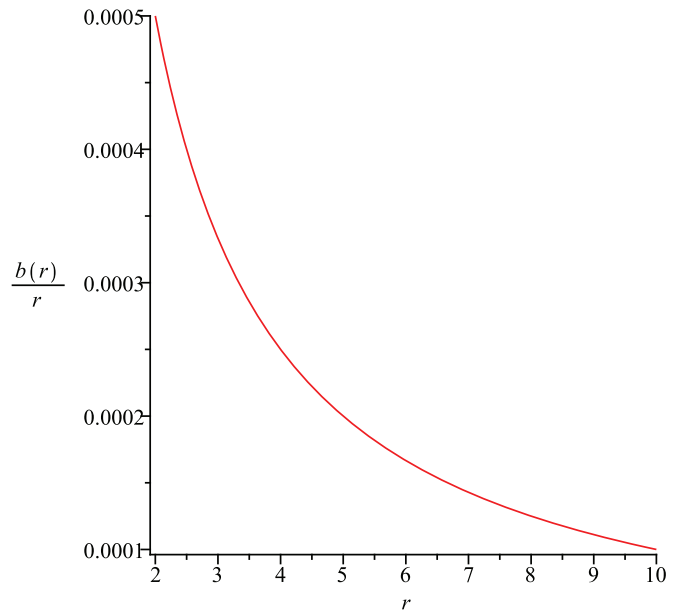
After using NFW DM density profile under the Einstein field equations, the shape function $b(r)$ is calculated ($8\pi = 1$) as

$$b(r) = 8\pi\rho_0[\ln(r) + C] \tag{24}$$

Note that C is the integration constant and it is chosen as

$$C = \frac{r_0}{8\pi\rho_0} - \ln r_0 \tag{25}$$

Fig. 7. $b(r)/r$ versus r ($r_0 = 0.001, \kappa = 1, \lambda = 1,$ and $\eta = -3/2$). [Colour online.]



Here Fig. 8 represents the shape function $b(r)$ and we see that the null energy condition ($\rho + p_r < 0$) is violated (see Fig. 9). Also we have checked the most important flare-out condition ($b(r) - r < 0,$ after the throat radius, i.e., $b' < 1$), which is satisfied and is plotted in Fig. 10.

Thus the generalized NFW DM profile that constitutes Dragonfly 44 can manage to provide a wormhole.

4.2. Case 2

In this case we choose $r_0 = 10, \rho_0 = 0.05,$ and $\gamma = 4$

After using NFW DM density profile under the Einstein field equations, the shape function $b(r)$ is calculated ($8\pi = 1$) as

Fig. 8. $b(r)$ versus r ($r_0 = 10$, $\rho_0 = 0.05$, and $\gamma = 3$). [Colour online.]

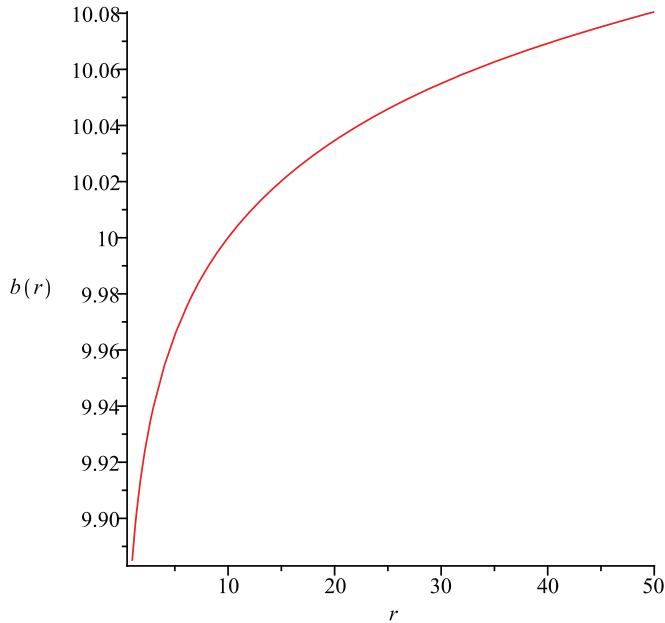


Fig. 10. $b(r) - r$ versus r ($r_0 = 10$, $\rho_0 = 0.05$, and $\gamma = 3$). [Colour online.]

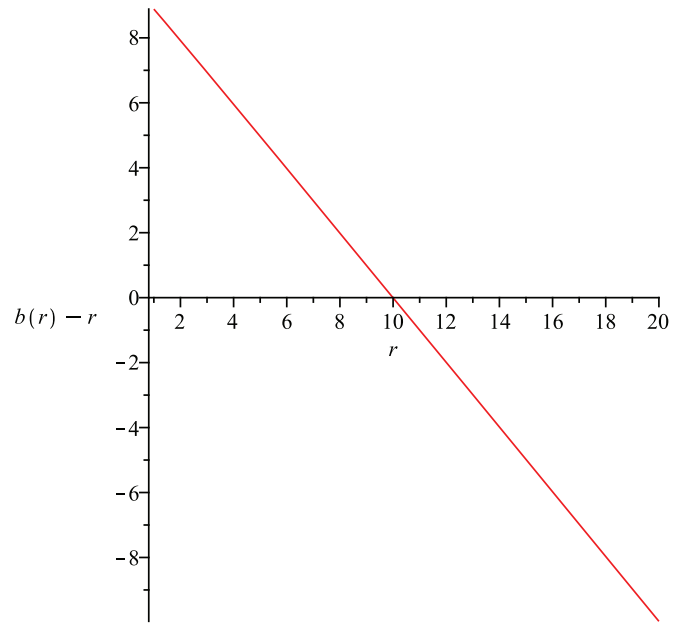


Fig. 9. Null energy condition for case 1 ($r_0 = 10$, $\rho_0 = 0.05$, and $\gamma = 3$). [Colour online.]

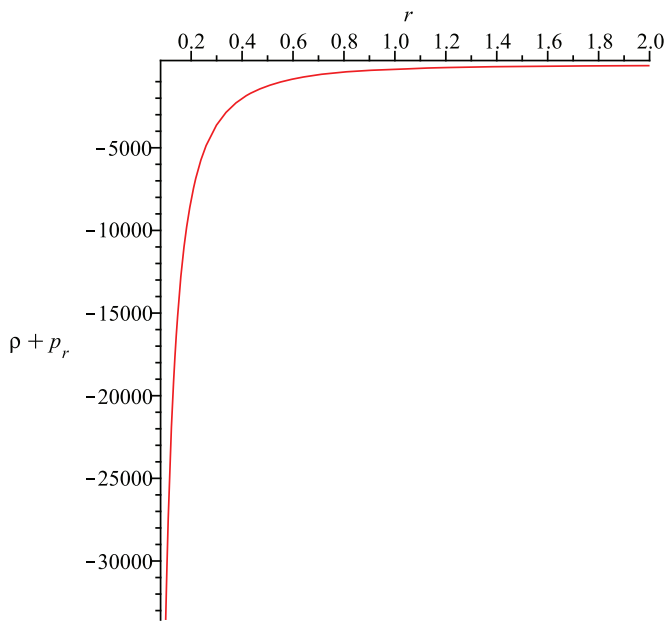
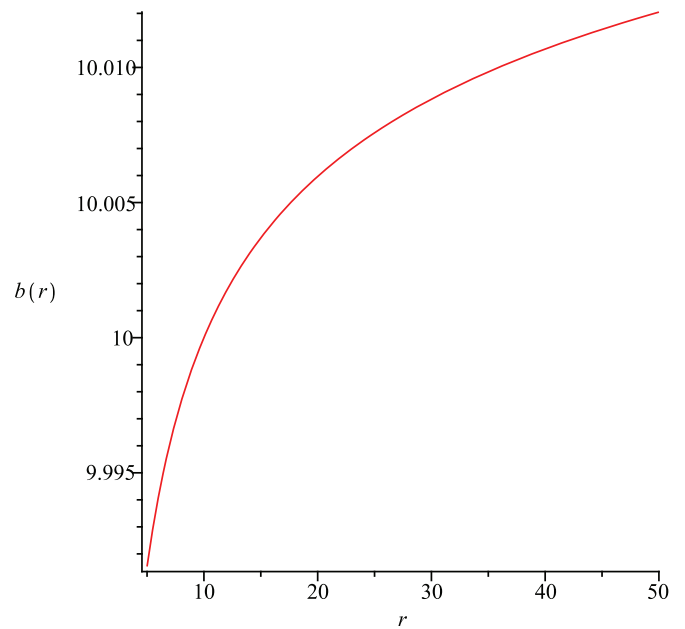


Fig. 11. $b(r)$ versus r ($r_0 = 10$, $\rho_0 = 0.05$, and $\gamma = 4$). [Colour online.]



$$b(r) = 8\pi\rho_0 \left[\frac{-1}{r} + \frac{\ln(r)}{r_0} + C \right] \tag{26}$$

Note that C is the integration constant and it is chosen as

$$C = \frac{r_0}{8\pi\rho_0} + \frac{1}{r_0} - \frac{1}{r_0} \ln r_0 \tag{27}$$

In this section we follow the same method used in case 1 and the shape function $b(r)$ is plotted in Fig. 11. To form a wormhole, the essential criteria regarding flare-out condition ($b(r) - r < 0$, after the throat radius, i.e., $b' < 1$) and violation of null energy condition ($\rho + p_r < 0$) are satisfied (see Figs. 12 and 13).

4.3. Case 3

In this case we assume $r_0 = 10$, $\rho_0 = 0.05$, and $\gamma = 5$.

After using NFW DM density profile under the Einstein field equations, the shape function $b(r)$ is calculated ($8\pi = 1$) as

Fig. 12. $b(r) - r$ versus r ($r_0 = 10$, $\rho_0 = 0.05$, and $\gamma = 4$). [Colour online.]

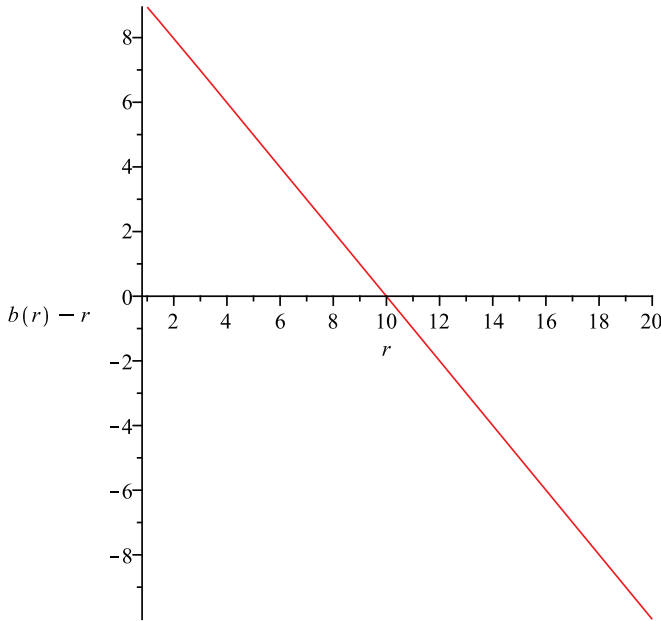
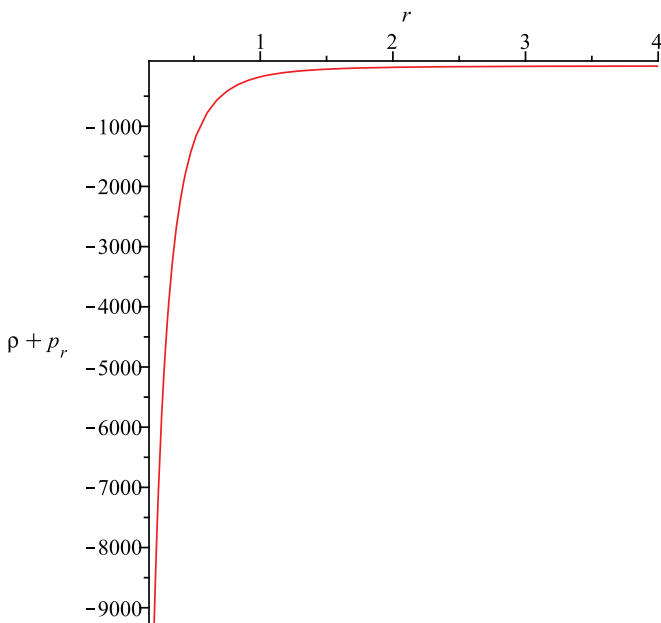


Fig. 13. Null energy condition for case 2 ($r_0 = 10$, $\rho_0 = 0.05$, and $\gamma = 4$). [Colour online.]



$$b(r) = 8\pi\rho_0 \left[\frac{-2}{rr_0} + \frac{\ln(r)}{r_0^2} - \frac{1}{2r^2} + C \right] \tag{28}$$

Note that C is the integration constant and it is chosen as

$$C = \frac{r_0}{8\pi\rho_0} + \frac{2}{r_0^2} - \frac{1}{r_0^2} \ln r_0 + \frac{1}{2r_0^2} \tag{29}$$

Fig. 14. $b(r)$ versus r ($r_0 = 10$, $\rho_0 = 0.05$, and $\gamma = 5$). [Colour online.]

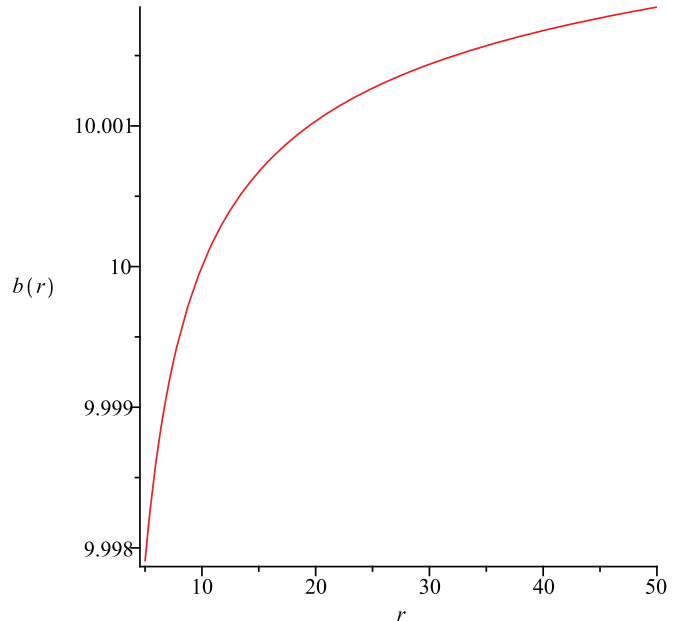
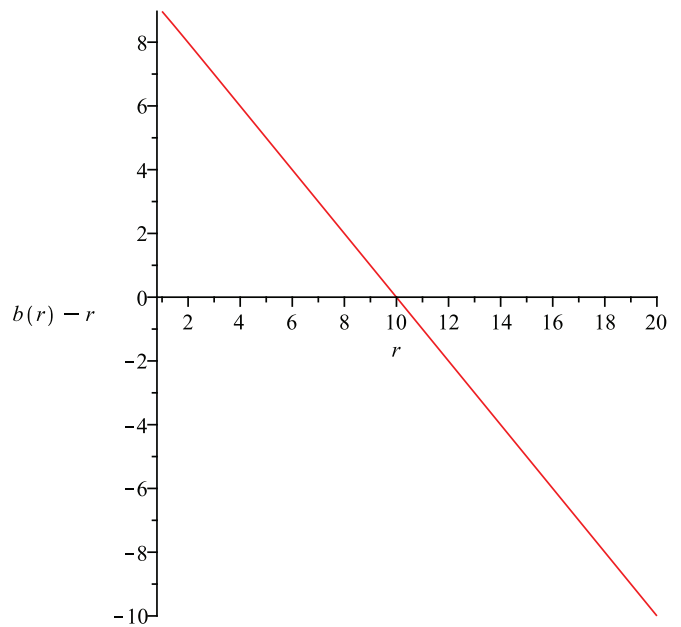


Fig. 15. $b(r) - r$ versus r ($r_0 = 10$, $\rho_0 = 0.05$, and $\gamma = 5$). [Colour online.]

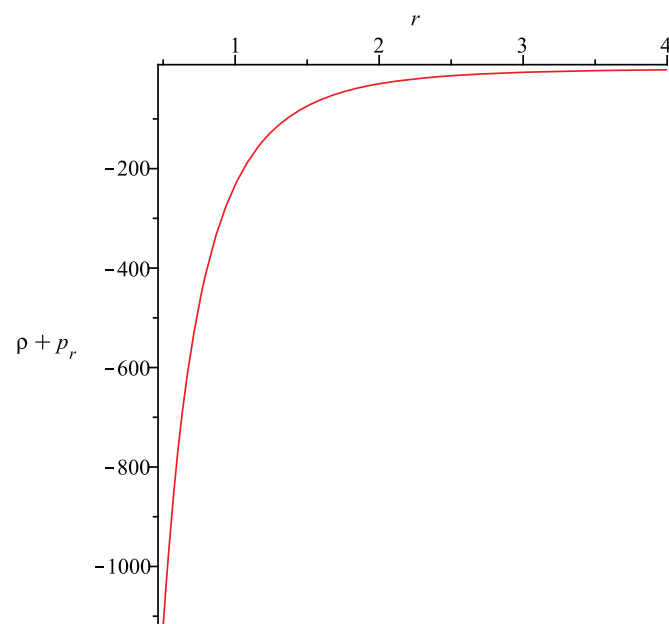


Here we use the same NFW DM density profile as the previous cases and similarly the shape function $b(r)$ is calculated and plotted in Fig. 14.

In Figs. 15 and 16, it is clearly shown that the flare-out condition ($b(r) - r < 0$, after the throat radius, i.e., $b' < 1$) is satisfied and null energy condition ($\rho + p_r < 0$) is violated to hold a wormhole open.

So we can claim that the generalized NFW DM profile that constitutes Dragonfly 44 provides a wormhole.

Fig. 16. Null energy condition for case 3 ($r_0 = 10$, $\rho_0 = 0.05$, and $\gamma = 5$). [Colour online.]



5. Conclusion

The presence of stable traversable wormholes is a noteworthy issue in theoretical physics. There is no doubt that wormholes are the most interesting objects in the universe. This work is inspired primarily by refs. 19–21. In this paper, we use the UDG systems in the Coma Cluster, which is known as Dragonfly 44, because astronomers reported that Dragonfly 44 may be made almost entirely of DM. Moreover, there is another possibility: in this study we show that this DM can form a wormhole, and it affects the observations. All the normal matter may be passed through this wormhole. For this purpose we firstly use the UDG profile and try to construct a wormhole solution, then we repeat our calculations for the NFW profile. We have shown that only NFW profile provides wormhole solutions. Thus we are able to find the solutions of the wormhole in the Dragonfly 44 galaxy so that the DM's halo around the Dragonfly 44 galaxy is suitable to harbor wormholes.

Acknowledgements

This work was supported by the Chilean FONDECYT Grant No. 3170035 (AÖ). AÖ is grateful to the CERN theory (CERN-TH) division for hospitality where part of this work was done. FR

would like to thank the authorities of the Inter-University Centre for Astronomy and Astrophysics, Pune, India, for providing research facilities. FR and SI are also grateful to DST-SERB and DST-INSPIRE, Govt. of India, for financial support respectively.

References

1. A. Einstein and N. Rosen. *Phys. Rev.* **48**, 73 (1935). doi:10.1103/PhysRev.48.73. PMID:10006752.
2. M.S. Moris and K.S. Thorne. *Am. J. Phys.* **56**, 395 (1988). doi:10.1119/1.15620.
3. M. Morris, K.S. Thorne, and U. Yurtsever. *Phys. Rev. Lett.* **61**, 1446 (1988).
4. M. Visser. *Lorentzian wormholes: From Einstein to Hawking*. Springer, Berlin, 1997.
5. M. Halilsoy, A. Ovgun, and S. Habib Mazharimousavi. *Eur. Phys. J. C*, **74**, 2796 (2014). doi:10.1140/epjc/s10052-014-2796-4.
6. F. Rahaman, M. Kalam, and S. Chakraborty. *Gen. Rel. Grav.* **38**, 1687 (2006). doi:10.1007/s10714-006-0325-y.
7. M.G. Richarte, I.G. Salako, J.P. Morais Graça, H. Moradpour, and A. Övgün. *Phys. Rev. D*, **96**, 084022 (2017). doi:10.1103/PhysRevD.96.084022.
8. S. Capozziello and M. Francaviglia. *Gen. Rel. Grav.* **40**, 357 (2008). doi:10.1007/s10714-007-0551-y.
9. M.S.R. Delgaty and R.B. Mann. *Int. J. Mod. Phys. D*, **4**, 231 (1995). doi:10.1142/S021827189500017X.
10. G.P. Perry and R.B. Mann. *Gen. Rel. Grav.* **24**, 305 (1992). doi:10.1007/BF00760232.
11. M. Cataldo and F. Orellana. *Phys. Rev. D*, **96**, 064022 (2017). doi:10.1103/PhysRevD.96.064022.
12. M. Cataldo, L. Liempi, and P. Rodriguez. *Phys. Lett. B*, **757**, 130 (2016). doi:10.1016/j.physletb.2016.03.057.
13. M. Cataldo, P. Labrana, S. Campo, J. del Crisostomo, and P. Salgado. *Phys. Rev. D*, **78**, 104006 (2008). doi:10.1103/PhysRevD.78.104006.
14. K. Jusufi, A. Övgün, and A. Banerjee. *Phys. Rev. D*, **96**, 084036 (2017). doi:10.1103/PhysRevD.96.084036.
15. I. Sakalli and A. Ovgun. *Eur. Phys. J. Plus*, **130**, 110 (2015). doi:10.1140/epjp/i2015-15110-9.
16. I. Sakalli and A. Ovgun. *Astrophys. Space Sci.* **359**, 32 (2015). doi:10.1007/s10509-015-2482-5.
17. A. Ovgun. *Eur. Phys. J. Plus*, **131**, 389 (2016). doi:10.1140/epjp/i2016-16389-6.
18. S. Kar, S. Lahiri, and S. SenGupta. *Phys. Lett. B*, **750**, 319 (2015). doi:10.1016/j.physletb.2015.09.039.
19. F. Rahaman, P.K.F. Kuhfittig, S. Ray, and N. Islam. *Eur. Phys. J. C*, **74**, 2750 (2014). doi:10.1140/epjc/s10052-014-2750-5.
20. F. Rahaman, P. Salucci, P.K.F. Kuhfittig, S. Ray, and M. Rahaman. *Ann. Phys.* **350**, 561 (2014). doi:10.1016/j.aop.2014.08.003.
21. A. Ovgun and M. Halilsoy. *Astrophys Space Sci.* **361**, 214 (2016). doi:10.1007/s10509-016-2803-3.
22. V. Sahni. *Lect. Notes Phys.* **653**, 141 (2004). doi:10.1007/978-3-540-31535-3_5.
23. J.L. Feng. *Annu. Rev. Astron. Astrophys.* **48**, 495 (2010). doi:10.1146/annurev-astro-082708-101659.
24. T.S.V. Albada, R. Sancisi, M. Petrou, and R.J. Tayler. *Phil. Trans. Roy. Soc. Lond. A*, **320**, 447 (1986). doi:10.1098/rsta.1986.0128.
25. C.R. Keeton, C.S. Kochanek, and E.E. Falco. *Astrophys. J.* **509**, 561 (1998). doi:10.1086/306502.
26. J.F. Navarro, C.S. Frenk, and S.D.M. White. *Astrophys. J.* **462**, 563 (1996). doi:10.1086/177173.
27. P. van Dokkum, R. Abraham, J. Brodie, C. Conroy, S. Danieli, A. Merritt, L. Mowla, A. Romanowsky, and J. Zhang. *Astrophys. J.* **828**, L6 (2016). doi:10.3847/2041-8205/828/l/L6.
28. I.R. King. *ApJL*, **174**, L123 (1972). doi:10.1086/180963.
29. A.N. Baushev. 2017. arXiv:1608.04356.